Repanas et al., Clin Exp Pharmacol 2015, 5:5
http://dx.doi.org/10.4172/2161-1459.1000192

Clinical & Experimental Pharmacology

Research Article Open Access

Coaxial Electrospinning as a Process to Engineer Biodegradable Polymeric Scaffolds as Drug Delivery Systems for Anti-Inflammatory and Anti-Thrombotic Pharmaceutical Agents

Alexandros Repanas[1*], Willem F. Wolkers[1], Oleksandr Gryshkov[1], Panagiotis Kalozoumis[2], Marc Mueller[1], Holger Zernetsch[1], Sotirios Korossis[2] and Birgit Glasmacher[1]

[1]*Institute for Multiphase Processes, Leibniz Universitat Hannover, Hannover, 30167, Germany*
[2]*Department of Cardiothoracic, Transplantation and Vascular Surgery, Hannover Medical School, Hannover, 30625, Germany*

Abstract

Objective: Blend electrospinning has been acknowledged as a cost-effective technique for the production of fibrous scaffolds, suitable for various biomedical applications. Coaxial electrospinning is a method variant that results in core-shell structures with advantages, such as delayed diffusion and protection of sensitive biomolecules. The aim of this work was to evaluate how different process and solution parameters affect the structural, mechanical and physical properties of the fibers, created by polycaprolactone (PCL). In addition, acetylsalicylic acid (ASA) that was used as a model anti-inflammatory and anti-thrombotic agent, was loaded within the fiber meshes in order to compare release kinetics between fibers produced by conventional blend and coaxial electrospinning.

Methods: Scanning electron microscopy (SEM) was used to investigate the structural and morphological characteristics of the fibers. The fibers' hydrophilicity was investigated using contact angle measurements while the electrical conductivity of the polymeric solutions and the thermal properties of the fibers were also evaluated. Differential scanning calorimetry (DSC) was used to determine the fibers' melting point and mechanical tensile tests were performed in order to study the mechanical properties of the fibers. Moreover, UV-vis spectroscopy was used to determine the release kinetics of ASA.

Results: The results indicated that increasing the concentration of PCL led to thicker and less aligned fibers. Furthermore, the physicochemical characterization did not reveal significant changes during the process. Coaxially electrospun fibers that were loaded with ASA exhibited a slower and sustained, biphasic release profile compared to blend electrospun fibers with 34% of ASA released during the first 8h and 97% in total after 3 months.

Conclusion: Taken together, fibrous meshes created by coaxial electrospinning using PCL, can be tailor-made by a careful optimization of all the process and solution parameters, in order to fit the scope of specific applications in the fields of biomedical engineering and drug delivery.

Keywords: Biomaterials; Fiber technology; Coaxial electrospinning; Polymers; Controlled drug delivery; Acetylsalicylic acid; Scaffolds

Introduction

During the past two decades electrospinning has received increased attention as a technology for applications in the biomedical field. It is an electrohydrodynamic technique that can be used to generate fibers or particles through an one-step process [1,2]. It utilizes electrical forces in order to create ultra-fine polymeric fibers from polymer melts, blends or emulsions [3]. In addition, it is a simple, cost-effective and versatile method that can be used to generate non-woven fiber meshes of different shapes and sizes [4]. Various solution parameters (concentration of polymers, choice of solvents, solution viscosity and surface tension) and process parameters (spinning distance, applied voltage and solution flow rate) affect the structural, physicochemical and mechanical properties of the fibers [5,6].

A typical design of an electrospinning apparatus has been described by Chronakis et al [7]. Two of the most important process parameters are the solution flow rate and the applied voltage. These parameters together with the spinning distance have to be carefully optimized in order to establish a stable and reproducible process. On the other hand, solution properties, such as viscosity and surface tension, which can be adjusted by the concentration of polymers and the choice of an appropriate solvent, determine the "electrospinnability" of a solution and the fundamental properties of the fibers that are generated. In contrast to blend electrospinning, coaxial electrospinning involves two concentrically arranged nozzles that are connected to the power source. This can be used to create fibers with a core-shell morphology that can have various applications in the fields of drug delivery, tissue engineering and wound healing [8-11]. Here, the application of two different solutions with different polymers and solvents can be used to create products with tailor-made properties if the process is properly controlled [12-14]. Polycaprolactone (PCL) is a hydrophobic, semi-crystalline polymer, approved from the Food and Drug Administration (FDA) in the United States of America, whose crystallinity depends on its molecular weight. It is easily soluble in most organic solvents, has a low melting point (59-64°C) and very good blend compatibility [15]. It presents numerous advantages, such as mechanical stability, slow degradation time (up to 3-4 years) and ability for long term controlled delivery of biomolecules of interest, such as drugs and proteins [16]. Additionally, the pore size of PCL scaffolds can be adjusted, in order to achieve proper cell seeding and tissue growth. Furthermore, the

***Corresponding author:** Alexandros Repanas, Leibniz Universitat Hannover Institute for Multiphase Processes Callinstrasse 36, 30167, Hannover, Germany, Tel: +49-0-511 762 3824; Fax: +49-0-511 762 3031; E-mail: repanas@imp.uni-hannover.de

Received: August 25, 2015; **Accepted:** September 21, 2015; **Published:** September 28, 2015

Citation: Repanas A, Wolkers WF, Gryshkov O, Kalozoumis P, Mueller M (2015) Coaxial Electrospinning as a Process to Engineer Biodegradable Polymeric Scaffolds as Drug Delivery Systems for Anti-Inflammatory and Anti-Thrombotic Pharmaceutical Agents. Clin Exp Pharmacol 5: 192. doi:10.4172/2161-1459.1000192

safety of PCL fibers in terms of cytotoxicity and biocompatibility has been demonstrated previously by several groups [4,17,18]. The fibrous scaffolds can be either produced under sterile conditions or be sterilized after their production using different methods. The combined properties hold great promise for potential applications in the field of drug delivery and tissue engineering [9,19–23].

The main focus of this study was to elucidate the effect of two process parameters (flow rate, applied voltage) and one solution parameter (PCL concentration), on the structural, mechanical and physical properties of PCL fibers generated via the coaxial electrospinning method, and to correlate the obtained data with previous research work in order to establish an optimized coaxial setup for the encapsulation of pharmaceutical agents for sustained delivery. In addition, acetylsalicylic acid (ASA) that was used as a model anti-inflammatory and anti-platelet drug, was encapsulated in the fiber meshes in order to compare the cumulative release between fibers created from coaxial and conventional blend electrospinning. ASA has been previously investigated as a thrombosis prevention factor in PCL tubular grafts [22]. The same polymer (PCL) and solvent were selected for both core and shell solutions in order to investigate the influence of the electrospinning method on drug release. The final aim of this work is to use the coaxial electrospinning technique as a means to confine the encapsulated drug close to the core of the fibers and reduce the initial burst effect, which is normally detected in drug delivery carriers fabricated by blend electrospinning, even though a core-shell structure was not given high priority. The findings of this study can be used to promote drug delivery systems (DDSs) for the sustained release of pharmaceutical agents in clinical applications related with cardiovascular diseases.

Materials and Methods

Materials

Polycaprolactone (PCL) (Mn = 70000-90000) and acetylsalicylic acid (ASA) (≥99.0%, crystalline) were purchased from Sigma-Aldrich. 2,2,2-trifluroethanol (TFE) was purchased from abcr GmbH & Co.KG. A phosphate buffer solution (PBS, pH = 7.4) was created in the lab using bi-distilled water. Ethanol (ROTIPURAN®, ≥99.8 % p.a., density = 0.79 g/cm3), used for the porosity measurements, was purchased by Carl Roth GmbH + Co. KG. All materials and reagents were used as received without further purification.

Polymer solution preparation and electrospinning

PCL was dissolved in TFE at a concentration of 150 mg/ml, for the samples of different flow rate and applied voltage, and at 120, 140, 160, 180 and 200 mg/ml for the samples of different concentration. All polymer solutions were left for 24h at room temperature under stirring (300 rpm) to achieve homogenous mixtures. The polymer solutions were then transferred to 10 ml syringes (Omnifix; B. Braun, Germany) while a portion of each was held for the electrical conductivity experiments. These syringes were used as the polymer reservoirs both for core and shell solutions. With the assistance of two software-controlled pumps (New Era Pump Systems Inc., USA) the polymer solutions were pumped out of their reservoirs at a constant rate of 4 ml/h for the samples of different applied voltage and PCL concentration and at rates of 1, 3 and 5 ml/h respectively for the different flow rate samples. Core and shell solution flow rates were the same, leading to a flow rate ratio of 1/1 for all samples. For the core solutions disposable blunt-tipped needles (Nordson EFD, USA) of an inner diameter of 0.8 mm were used while the inner diameter of the coaxial spinneret nozzle for the shell solution was 1.35 mm. The distance between the tip of the coaxial nozzle and the surface of the collector was kept constant at 25 cm for all samples. A collector that constantly rotated at 1000 rpm (150 mm diameter and 50 mm width), covered with an aluminum foil was used to collect the samples. A constant high voltage (25 kV) was used via a power source (Matsusada, Precision Inc., Japan) for the samples with different flow rate and PCL concentration. On the other hand, applied voltage of 17, 19, 21, 23 and 25 kV for the samples with different voltage, was applied at the nozzle to charge the solution. The initial droplet, formed at the tip of the nozzle due to the solution been pumped, was elongated when the charge-charge repulsions created from the applied voltage overcame the solution's surface tension. This subsequently led to the formation of a jet that was accelerated towards the collector while the solvent got evaporated before the jet reached the surface, thus, creating fibers that were deposited on the aluminum foil. Electrospinning was performed under constant conditions of temperature and relative humidity (T=23 ± 1°C, Rel. Humidity = 40 ± 3 %). The samples were then collected and left to dry overnight under vacuum. For the production of electrospun fibers with ASA, a core solution of 15 mg/ml ASA and 150 mg/ml PCL as a blend in TFE and a shell solution of 150 mg/ml PCL in TFE were used. The solutions were left for 24h at room temperature under stirring (300 rpm) to achieve homogenous mixtures. A similar set of process parameters was used to create the fiber mats (applied voltage = 25 kV, nozzle to collector distance = 25 cm, core solution flow rate = 1 ml/h, shell solution flow rate = 3 ml/h, rotating collector's speed = 1000 rpm). PCL fibers with encapsulated ASA using conventional blend electrospinning were also electrospun to serve as a control.

Characterization of electrospun fiber mats

Electrical conductivity: The electrical conductivity of the polymeric solutions was measured using a conductometer (SevenMulti, Mettler Toledo AG). Five milliliter of each different polymer solution was measured at 25°C. All measurements were performed in quintuplicates.

Scanning electron microscopy (SEM): Square samples of 5×5 mm^2 were cut from each different sample and were sputter coated with Au/Pd for 60s before been placed inside the SEM instrument (S3400N. Hitachi, Japan). A high voltage of 15 kV and a tip to sample distance of 7 mm were used to examine the samples. Magnifications of 500ˣ, 1000ˣ, and 4000ˣ were used both for quantitative and qualitative analysis. For the fiber diameter, alignment and pore size measurements pictures were analyzed with ImageJ software (National Institutes of Health, USA). Measurements were taken at 50 different fibers from each sample.

Water contact angle assay: Square strips of 10ˣ10 mm2 were cut from each different sample and static contact angles of fiber mats were measured using an optical contact angle apparatus (FM40 Easydrop, Krüss, Germany) at room temperature. Measurements were taken at 0s after the droplet of bi-distilled water (1 μL) touched the surface of the samples. Photos at 0s were taken for the samples with different PCL concentrations. The contact angle data was calculated by the software that accompanied the apparatus. The experiments were performed in quintuplicates.

Mechanical testing: Rectangular samples of 15 mm gauge length and 10 mm width were carefully cut from each different sample. The thickness of each specimen was measured with a thickness gauge (Quick mini, Mituotoyo). Duct tape was carefully placed at each edge of the samples to improve the mounting on the pneumatic grips of the testing device. Uniaxial tensile tests were conducted on an INSTRON 5967 Dual Column tensile testing machine with a 100 N load cell (Instron, USA). Ultimate tensile strength (UTS), strain at the maximum force,

Young's modulus (linear slope of the stress/strain curve) and Toughness were measured and analyzed (Blue-Hill software, Instron, USA). All experiments were done at room temperature. A strain rate of 20 mm/min was used. All samples were elongated until failure. Experiments were performed in sixtuplicates.

Differential scanning calorimetry (DSC): Analyses using differential scanning calorimetry (DSC) were performed using a Netzsch DSC 204 F1 Phoenix instrument (Netzsch Geratebau GmbH, Selb, Germany). Calibration was done using Adamantan ($C_{10}H_{16}$), In, Sn, Bi, Zn, and CsCl as standards. Approximately 5 mg of the fiber samples were transferred into 25 µL aluminum pans, which were hermetically sealed and placed in the DSC. Samples were heated from -100 to 100°C with 10 K min^{-1}, while monitoring the heat flow. An empty pan was used as a reference.

Netzsch Proteus thermal analysis software (Netzsch Geratebau GmbH, Selb, Germany) was used to analyze the obtained thermograms. The onset and midpoint temperature (T_{onset} and T_{peak} in°C) were determined. This was done by determining the temperature at the intersection of the baseline of the thermogram and upward slope of the peak and temperature at the peak maximum, respectively. The enthalpy of the thermal event (Δ H in J g^{-1}, where the weight represents the fresh weight of the tissue sample) was determined from the baseline-corrected area under the peak.

Porosity measurements: The porosity of the specimen types that were used in the drug release studies was evaluated by the liquid displacement method [24,25]. A cylinder containing a predetermined volume of ethanol (V1) was used to immerse the scaffolds. The specimens were kept in ethanol for 15 min to allow it to penetrate and fill the scaffolds' pores. The total volume of ethanol with the immersed scaffold was determined (V2). After this, the scaffolds were removed from the cylinder in order to determine the residual volume of ethanol (V3). Equation 1 (Eq. 1) was used to calculate the porosity (%):

$$P_{\%} = (V1-V3) / (V2-V3) \quad \text{- (Eq. 1)}$$

***In vitro* drug release:** Samples that were punched out from both coaxially spun and blend electrospun scaffolds were weighed, immersed in 20 ml of PBS and kept in an incubator at 37°C. At predetermined time points, small aliquots of solution were taken for measuring the light absorbance in a UV-Vis spectrometer and added back to the solution. Using a UV-Vis spectrometer (LIBRA S22, Biochrom, Germany), the concentrations of both ASA and salicylic acid (SA) in the solution was determined by measuring the absorbance at 267 and 296 nm, respectively. The SA amount in the solution had to be determined because ASA is hydrolyzed into SA and acetic acid in PBS [26]. Standard calibration plots of concentration versus absorbance were created to determine the ASA and SA concentrations in the samples. The amount of ASA released in the solution was calculated according to (Eq. 2) [22].

$$ASA_{solution} = [SA]_{solution} \times V_{solution} \times MW_{ASA}/MW_{SA} \quad \text{- (Eq. 2)}$$

Where $V_{solution}$ stands for the volume of the measured solution and MW_x for the molecular weight of ASA and SA respectively.

In order to calculate the percentage of the released drug over time, the ratio between the cumulative amount of ASA released in the solution and the amount of ASA that was initially loaded into the fibers was calculated according to (Eq. 3):

$$ASA\% = ASA_{solution}/ASA_{sample} \times 100 \quad \text{- (Eq. 3)}$$

The initial amount of ASA in the fibers was calculated by cutting samples that were afterwards weighed and immersed in TFE. The samples were immediately dissolved and the concentration of ASA was measured as described above. All experiments were carried out in triplicates.

Statistical analysis

All data are expressed as mean ± standard deviation unless otherwise noted. One-way analysis of variance (ANOVA) with post hoc Tukey means comparison tests were conducted and p values < 0.05 were considered significant.

Results and Discussion

Morphology and structure of fibers

Three different parameters during polymer solution preparation and electrospinning were examined for their effect on the structural, physical and mechanical properties of the generated fibers. In Figure.1A, SEM pictures depict the differences between the electrospun fibers for different solution flow rate, applied voltage and PCL concentration. In all cases smooth, cylindrical, bead-less fibers were created that formed dense fiber networks. In the first column of Figure 1A, fibers with different flow rate are depicted. In addition, in the middle and right column of the same Figure, electrospun fibers with different applied voltage and different PCL concentration are shown, respectively. Depended on the operational parameters the fibers average diameter and alignment was influenced, as it can be seen from Figure 1A. However, due to the fact that the parameter that was kept constant each time for each different set of samples was not the same between specimens created for each parameter study, a cumulative comparison of all of them was not possible in the current study. Instead, each parameter was individually assessed. In Figure.1B the alignment of the electrospun fibers on the surface of the collector was depicted. In case of different flow rates, the standard deviation of the fiber alignment values raised from 5.98° (1 ml/h) to 14.36° 5 ml/h). This could indicate that increasing flow rates result in less aligned fibers. Similarly, increasing applied voltage values led to an increase in the standard deviation of fiber alignment, from 6.12° (17 kV) to 10.33° (25 kV). The fiber alignment also dropped when higher concentration of PCL were used (SD = 4.89, PCL concentration = 120 mg/ml compared to SD = 20.99, PCL concentration = 200 mg/ml). The data summarized in Table 1 show that the average fiber diameter increased with an increase in the solution flow rate and PCL concentration from 1.80 ± 0.47 µm (1 ml/h) to 2.33 ± 0.45 µm (3 ml/h) and from 1.01 ± 0.33 µm (120 mg/ml) to 3.37 ± 0.39 µm (200 mg/ml), respectively. The data sets are in agreement with previous studies [27,28] resembling the effects that have been investigated in conventional blend electrospinning. The higher flow rate resulted in the presence of higher amounts of the polymeric fluid in the jet, which increased the average fiber diameter. Moreover, increased polymer concentration and thus solution viscosity resulted in larger average fiber diameters because the elongation of the jet required more time and effort. On the other hand, applied voltage initially led to an increase in average fiber diameter until 21 kV from 1.96 ± 0.77 µm (17 kV) to 2.25 ± 0.51 µm (21 kV). For higher voltage values the fiber diameter did not increase further and the differences in the average values were statistically insignificant (p>0.05). In several studies it was concluded that a higher applied voltage leads to increased ejection of polymer fluid in a jet but there have been also reports of initial decrease in fiber diameter [29-31]. During electrospinning, the spinning distance was kept constant at 25 cm. Therefore the electrical field generated was mainly affected by the applied voltage. It could be possible that changing the spinning distance would result in different electrical field which in turn would have influenced the properties of

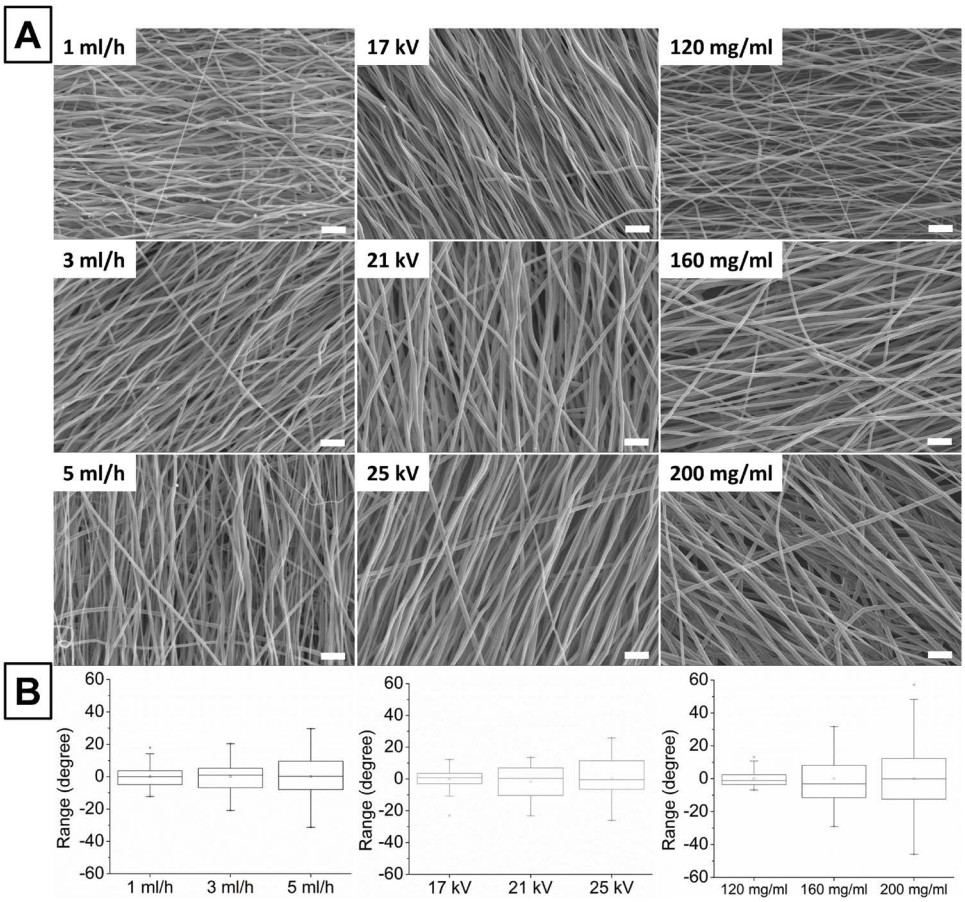

Figure. 1. SEM images of electrospun fiber mats at different set of parameters; flow rate (first column), applied voltage (second column), PCL concentration (third column); magnification = 500x, scale bars = 20 μm (A). Fiber alignment box charts for the different set of parameters (B); n = 50, mean ± SD.

the fibers.

The electrical conductivity of the polymer solutions is depicted in Table 1. Increased PCL concentration led to a decrease in electrical conductivity of the solutions from 0.85 ± 0.04 μS/cm (120 mg/ml) to 0.40 ± 0.01 μS/cm (200 mg/ml). The electrical conductivity values of the samples that were electrospun under different applied voltage and flow rate remained the same as expected since they all came from the same solution. From the data in the table it can be concluded that a decrease in electrical conductivity leads to an increase in average fiber diameter which has been previously reported in other studies [5,12,27,32].

Water contact angle

Static contact angle measurements were conducted in order to study the surface differences between the different mats with all experiments performed under the same conditions (Figure 2). Results showed that an increase in each of the three parameters led to an increase in the angle of the water drop in the surface of the fibers. The static contact angle in all cases did not exceed 90° and the surfaces can be considered as relatively hydrophilic. The statistical analysis showed significant difference in the values of the contact angle between flow rates of 1 and 5 ml/h. More specifically, fibers created with 1, 3 and 5 ml/h flow rate exhibited an average static contact angle of 77.66 ± 2.04°, 82.18 ± 3.34° and 84.58 ± 2.60°, respectively. Moreover, samples created with applied voltage of 17 kV (64.90 ± 3.55°) significantly differed from samples created with applied voltage of 23 (74.18 ± 1.73°) and 25 kV (78.84 ± 4.96°), respectively. Finally, statistically significant differences were detected when PCL concentration variance was more than 20 mg/ml. More specifically, sample 120 mg/ml (69.58 ± 2.44°) statistically differed from samples 160 mg/ml, 180 mg/ml and 200 mg/ml ($p<0.05$). Additionally sample 140 mg/ml (71.04 ± 2.10°) statistically differed from samples 180 mg/ml and 200 mg/ml ($p < 0.05$). Finally, samples 160 mg/ml (74.78 ± 2.56°) and 200 mg/ml (81.90 ± 1.90°) were also statistically different ($p < 0.05$).

The ability to control the surface's reaction with liquid media is very important for drug delivery applications. A surface that would enable quick water uptake and infiltration to the inner parts would result in a faster release of the pharmaceuticals through the matrix due to diffusion. On top of that, this could result in a burst release of the pharmaceuticals during the first hours, which is undesirable for sustained drug release applications. The nature of the encapsulated pharmaceuticals also plays a crucial role in the release kinetics. Water-soluble and water- insoluble pharmaceuticals display different release kinetics. On the other hand, a less hydrophilic surface could result in an initial delay of diffusion of the molecules via the polymeric matrix. Therefore, it was important for this study to investigate a way to manipulate the release behavior through changes in the structural and physical properties of the fibers, induced by parameter optimization.

Citation: Repanas A, Wolkers WF, Gryshkov O, Kalozoumis P, Mueller M (2015) Coaxial Electrospinning as a Process to Engineer Biodegradable Polymeric Scaffolds as Drug Delivery Systems for Anti-Inflammatory and Anti-Thrombotic Pharmaceutical Agents. Clin Exp Pharmacol 5: 192. doi:10.4172/2161-1459.1000192

Sample	Fiber diameter	Electrical conductivity	Ultimate tensile strength (UTS)	Tensile strain at F_{max}	Young's modulus	Toughness
	mean ± SD μm	mean ± SD μS/cm	mean ± SD MPa	mean ± SD mm/mm	mean ± SD MPa	mean ± SD MJ/m^3
1 ml/h	1.80 ± 0.47	0.52 ± 0.01	4.30 ± 0.61	3.70 ± 0.49	27.93 ± 2.95	15.02 ± 1.98
3 ml/h	2.08 ± 0.40	0.52 ± 0.01	10.09 ± 1.40	0.86 ± 0.02	42.62 ± 3.79	12.87 ± 2.47
5 ml/h	2.33 ± 0.45	0.52 ± 0.01	12.96 ± 1.93	0.66 ± 0.02	47.01 ± 4.19	10.35 ± 1.73
17 kV	1.96 ± 0.77	0.52 ± 0.01	13.64 ± 1.73	0.89 ± 0.05	55.73 ± 3.50	21.53 ± 1.26
19 kV	2.15 ± 0.61	0.52 ± 0.01	9.63 ± 1.05	0.88 ± 0.06	50.81 ± 4.08	19.12 ± 1.09
21 kV	2.25 ± 0.51	0.52 ± 0.01	7.80 ± 2.26	0.82 ± 0.03	38.87 ± 5.22	16.72 ± 0.98
23 kV	2.26 ± 0.41	0.52 ± 0.01	6.99 ± 0.89	0.75 ± 0.03	36.07 ± 5.27	14.50 ± 1.43
25 kV	2.22 ± 0.55	0.52 ± 0.01	5.98 ± 0.59	0.74 ± 0.04	30.29 ± 2.43	12.40 ± 1.33
120 mg/ml	1.01 ± 0.33	0.85 ± 0.04	9.33 ± 1.30	0.62 ± 0.07	35.30 ± 5.22	7.55 ± 1.34
140 mg/ml	1.36 ± 0.40	0.66 ± 0.03	7.72 ± 2.39	0.67 ± 0.06	32.55 ± 6.11	10.57 ± 1.20
160 mg/ml	2.03 ± 0.41	0.48 ± 0.02	5.80 ± 1.04	5.35 ± 0.32	28.11 ± 6.18	13.90 ± 2.10
180 mg/ml	2.44 ± 0.36	0.41 ± 0.01	4.78 ± 0.80	5.81 ± 0.28	22.77 ± 5.30	19.24 ± 1.40
200 mg/ml	3.37 ± 0.39	0.40 ± 0.01	4.10 ± 1.94	6.25 ± 0.30	19.94 ± 3.01	25.79 ± 1.82

Table 1: Summary of structural (average fiber diameter), physical (electrical conductivity), and mechanical properties (ultimate tensile strength, tensile strain at maximum force, Young's modulus and Toughness) of the electrospun fibers.

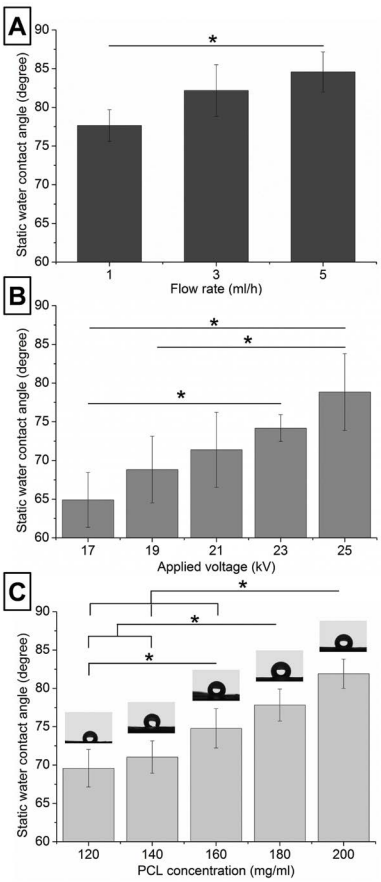

Figure. 2. Influence of the flow rate (A), applied voltage (B) and PCL concentration (C) on the water static contact angle formed on the surface of the samples; n = 5, mean ± SD.

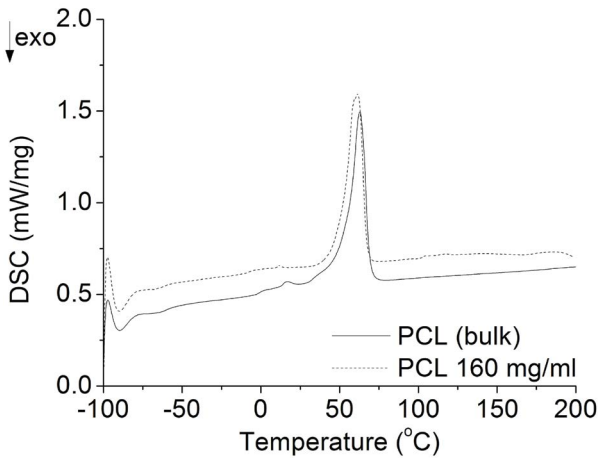

Figure. 3. DSC thermograms of a 160 mg/ml PCL scaffold (black dashed line) and bulk PCL (black solid line) from -100 oC up to 200 oC. The melting points Tm (62.8 oC for PCL bulk, 61.3 oC for the PCL scaffold) as well as the glass transition points Tg (-61.2 oC for both) can be identified for both the bulk material and the scaffold.

DSC experiments

The thermograms of bulk PCL pellets and electrospun fibers of 160 mg/ml PCL are depicted in Figure 3. PCL is a semi-crystalline polymer with melting temperature (T_m) of around 60°C and glass transition temperature (T_g) at around – 60°C [33]. Both bulk PCL and electrospun fibers had a T_g of -61.2°C. Additionally, the T_m decreased from 62.8°C for the pellets to 61.3°C for the electrospun fibers (PCL concentration: 160 mg/ml). The latter could be attributed to decreased crystallinity of the PCL fibers, occurred during the electrospinning process [33,34]. Moreover, the bulk PCL that was used was not 100% purified and there might have been also some impurities introduced in the fibers from the parts of the electrospinning set-up during the process. In fact, in the bulk thermogram there was a small peak visible at around 20°C and glass transitions at 0°C were visible for both thermograms of PCL fibers and bulk PCL. The data from DSC showed that the electrospun scaffolds do not display significant chemical changes during the process and their properties remain similar to bulk PCL.

Mechanical characterization

Table1 summarizes all mechanical testing data. Increasing values of solution flow rate led to increased values of UTS (from 4.3 ± 0.61 MPa for 1 ml/h to 12. 96 ± 1.93 MPa for 5 ml/h) (Figure 4A). On the other hand, increasing values of applied voltage generated fibers with lower average UTS (Figure 4B). The values decreased significantly ($p<0.05$)

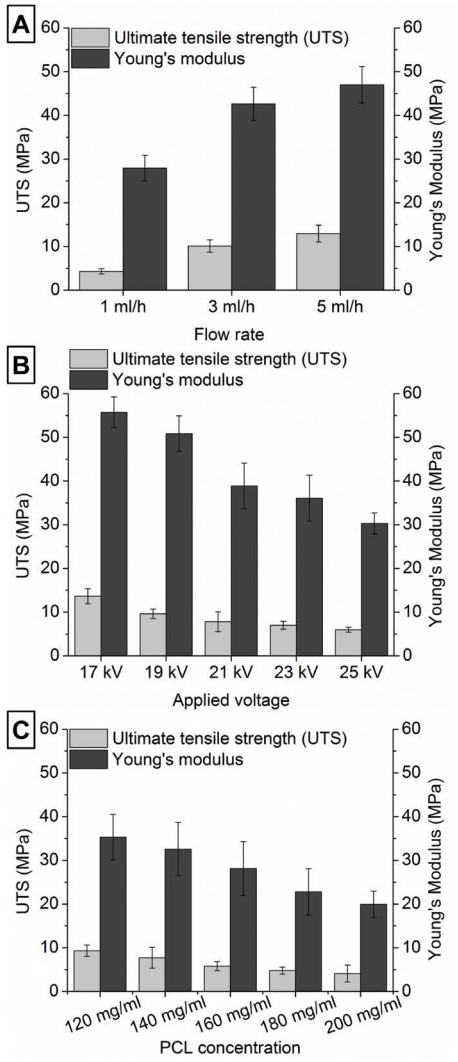

Figure. 4. Mechanical properties of electrospun PCL scaffolds at different parameter set-ups. Young's modulus and tensile stress at maximum load comparative graphs for different flow rate (A), different applied voltage (B) and different PCL concentration (C); n = 6, mean ± SD.

until 21 kV (from 13.64 ± 1.73 MPa for 17 kV down to 7.8 ± 2.26 MPa for 21 kV) and then further decreased but with a lower rate until 25 kV (from 7.8 ± 2.26 MPa down to 5.98 ± 0.59 MPa). For the samples with different PCL concentrations the ultimate tensile strength values decreased from 9.33 ± 1.30 MPa for the 120 mg/ml samples down to 4.1 ± 1.94 MPa for the 200 mg/ml samples (Figure 4C). It can be concluded that the average diameter and the alignment of the fibers have a different impact on the average UTS values. In case of different flow rates, the UTS values coincides with the increase in the average fiber diameter, whereas in case of the applied voltage and the concentration of PCL, the average UTS dropped when the deviation of the alignment of the fibers was higher, in agreement with the data that were presented in chapter 3.1.

Tensile strain values at maximum load were within the range of 0.62 – 0.89 mm/mm for all samples with the exception of 1 ml/h flow rate sample and the ones with more than 160 mg/ml PCL concentration. In the first case, tensile strain remarkably exceeded 3.7 ± 0.49 mm/mm. It is possible that the slow rate of polymer solution deposition on the collector resulted in a more favorable macroscopic structure with fibers

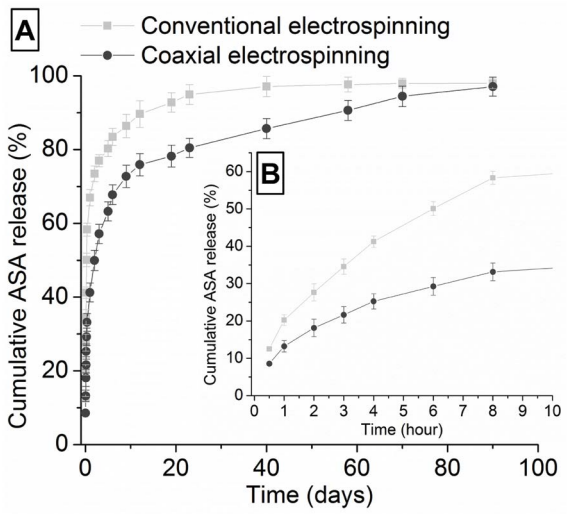

Figure. 5. The cumulative release of the drug from the electrospun fibers was plotted as a function of time. The error bars represent the standard deviation values from the tests. Cumulative ASA release from fibers created with coaxial and conventional electrospinning during the first 90 days(A) and the first 8 Hours (B) respectively; n=3, mean ± SD.

that can be elongated more than 3.5 times their length until failure. This can be a very interesting feature for applications that require scaffolds with high elongation capacities. In the case of fibers produced with more than 160 mg/ml PCL concentration, the tensile strain reached the remarkable value of 6.25 ± 0.30 mm/mm for the 200 mg/ml samples. Similar behavior has been identified for PCL single jet fibers with gradient PCL concentration [35].

Young's modulus values calculated from the linear slope of the stress-strain curves exhibited similar trends with UTS. In the case of increasing values of applied voltage and PCL concentration where increased deviation in the fiber alignment was observed (Figure 1B), the average Young's modulus values decreased (Figure 4B & C). More specifically, Young's modulus values dropped from 55.73 ± 3.5 MPa for the 17 kV samples down to 30.29 ± 2.43 MPa for the 25 kV samples, and from 35.3 ± 5.22 MPa down to 19.94 ± 3.01 MPa for the 120 mg/ml and 200 mg/ml samples, respectively. On the other hand, increasing flow rate led to increased Young's modulus and increased fiber diameter values (Figure 4A). Statistical analysis showed that Young's modulus values of the different flow rate samples were statistically different ($p < 0.05$). Additionally, only samples that were generated with a more than 2 kV voltage difference were found statistically different ($p < 0.05$). Moreover, PCL concentration of 160 mg/ml was found to be important since significant differences in Young's modulus values were only found between the samples with concentrations below and above that limit. Other groups have also studied how parameters such as polymer concentration can influence fiber diameter and alignment and eventually the mechanical properties [36]. However, fiber alignment is a parameter that needs to be carefully addressed, both qualitatively and quantitatively in order to precisely determine the influence of the scaffolds' micro-architecture on the mechanical properties. Additionally, the micro-architecture of an electrospun scaffold that would be used as a carrier for pharmaceuticals could influence their release. Hence, it was crucial to determine if the architecture can be controlled sufficiently through parameter optimization. A comparison with values from the literature is difficult because of the nature of the

testing processes and the different protocols that can be followed. Furthermore, toughness is another important mechanical property for the fabricated materials opted for biomedical applications [37,38]. The obtained values are summarized in Table 1. The average toughness slightly reduced from 15.02 ± 1.98 MJ/m3 (1 ml/h) to 10.35 ± 1.73 MJ/m3 (5 ml/h) ($p>0.05$) and from 21.53 ± 1.26 MJ/m3 (17 kV) to 12.40 ± 1.33 MJ/m3 (25 kV) ($p < 0.05$). On the other hand, the average toughness of the samples created with different PCL concentration significantly increased from 7.55 ± 1.34 MJ/m3 (120 mg/ml) to 25.79 ± 1.82 MJ/m3 (200 mg/ml) ($p < 0.05$), being comparable with values from previous studies, performed with similar materials [37,38].

In vitro drug release study

The cumulative release profiles of ASA incorporated in the fabricated fibers using both electrospinning methods are shown in Figure 5. The cumulative amounts of ASA were calculated as the release fraction of the total ASA content entrapped within the fibers in PBS medium (pH 7.4). The study was carried out in an incubator at 37 °C over a period of 90 days. Before discussing the obtained results, an investigation over the structural and morphological parameters of the scaffolds, such as the average porosity and pore size as well as the average fiber diameter, had to be performed in order to compare appropriately the two electrospinning variants. The average pore size for the blend and coaxially electrospun fibers was 7.04± 3.71 μm and 6.80± 2.70 μm, respectively ($p>0.05$). Moreover, the average porosity values for the blend and coaxial scaffolds were 84.72± 2.76 % and 86.35± 1.46%, respectively ($p>0.05$). In addition, the use of the coaxial method led to a decrease in the average fiber diameter from 0.85± 0.35 μm for the blend fibers to 0.80± 0.30 μm, which was not significant ($p>0.05$). Taken together, the morphological and structural analysis of both electrospun fibrous scaffolds did not reveal any significant changes in the fibers' characteristics and therefore a direct comparison between the drug's release kinetics from both formulations was possible.

There are two major mechanisms that can determine the release of drugs from biodegradable polymeric formulations. The first mechanism is driven by polymer degradation and the second through small molecule diffusion [39]. According to Woodruff et al., there is no evidence reported for significant PCL degradation in such a period of time [11]. Thus, it was expected that diffusion through the polymeric matrix would be the predominant mechanism for ASA release [40]. After 90 days inside the surrounding medium, almost 98% of the total amount of ASA was released from the fibers created by blend electrospinning and 97% of the fibers created by coaxial electrospinning (Figure 5A). Furthermore, in both cases, a biphasic release profile can be observed. During the first stage ASA molecules that are present on the surface or near it, quickly diffuse to the release medium. The use of the coaxial method was considered to ensure that the vast amount of ASA would be encapsulated inside the core. Nevertheless, because the same polymer and solvent were used in the core and shell solutions, a possible mix at the tip of the nozzle during electrospinning might have caused a part of ASA to be also present in the shell solution and therefore near or at the surface of the fibers. A distinct core-shell structure was not the case for the fibers created with the coaxial approach due to the set-up. Another explanation could be the semi-crystalline nature of PCL. Kim et al. proposed that the latter was the reason of forcing drug aggregates to the surface of the electrospun fibers during the electrospinning process [16]. In addition, PCL fiber mats, that were created using blend electrospinning, displayed an immediate release of ASA that reached almost 60% of the total amount of the drug during the initial 8h (Figure 5B). On the other hand, this burst effect was lower in the case of the coaxially spun fibers, where ASA was expected to be mainly encapsulated in the core of the fibers. In this case, the release of ASA almost reached 34% during the initial 8h (Figure 5B). In both cases the initial burst release was followed by a sustained release period that lasted until the end of the experiment. During the second stage of the release profile, the coaxially spun fibers resulted in a more gradual release through time. At day 45, which was the middle point of the study, the cumulative release of ASA reached almost 85% while the amount released from the conventional blend electrospun fibers was already more than 97%. During this stage, the ASA molecules that were encapsulated deeper inside the fibers had to diffuse through longer distances inside the polymeric matrix. In the case of coaxially spun fibers, a considerable amount of ASA molecules are expected to be distributed mainly near the core and therefore would require longer time to diffuse. This could explain the differences in the release profiles between the methods and also support the hypothesis that coaxially spun fibers are more suitable for sustained release of pharmaceuticals over time, even if a clear core-shell structure could not be achieved. Moreover, fiber diameter seems to play an important role in this matter since it can influence the time the molecules need to diffuse through the matrix, making it a crucial property to control through the optimization of the aforementioned solution and process parameters. Del Gaudio et al. presented similar results for the same time periods, with total study duration of one week [22]. In addition, several other groups including Zhang et al. and Yan et al. have presented results indicating the suitability of electrospun fibers for prolonged release of pharmaceuticals [9,20,23].

Conclusion

PCL fibrous meshes were created using the coaxial electrospinning technique. The main goal of this work was to determine if by controlling different parameters before and during electrospinning a prediction or adjustability of the final products could be achieved. Results showed that different solution and process parameters affect the structural and mechanical properties of the fibers in a similar manner as during blend electrospinning. Polymer concentration is one of the most important parameters. Increased PCL concentration led to thicker, less aligned fibers and applied voltage had similar effects. DSC results showed that there were only minor visible changes between the electrospun scaffolds and PCL in bulk form. In addition, the mechanical studies showed that varying structural properties through changes in process and solution parameters can greatly affect the tensile stress the fibers can withstand when maximum load is applied. Moreover, coaxially spun fibers showed a more sustained release profile of ASA compared to fibers created by blend electrospinning, leading to the conclusion that they would be more suitable as drug delivery carriers, even without having a distinct core-shell morphology. Summarizing, the results of this study show that PCL electrospun fibers can be methodically and easily modified to obtain desired properties through a careful and well-designed optimization of the parameters that influence the initial preparation of the polymeric solutions as well as the process itself. Hence, PCL electrospun fibers are promising candidates as scaffolds for sustained drug delivery applications.

Acknowledgement

This research was granted by the German Research Foundation (DFG) by the Cluster of Excellence REBIRTH (From Regenerative Biology to Reconstructive Therapy, DFG EXC 62/1).The authors express their sincere gratitude to fellow researcher Lothar Lauterboeck MSc. from the Institute for Multiphase Processes, Leibniz Universität Hannover, as well as Poulami Basu MTech. from the Biomedical Engineering Division, Vellore Institute of Technology, Vellore, India, for their individual contributions to the experimental procedures and manuscript editing.

Citation: Repanas A, Wolkers WF, Gryshkov O, Kalozoumis P, Mueller M (2015) Coaxial Electrospinning as a Process to Engineer Biodegradable Polymeric Scaffolds as Drug Delivery Systems for Anti-Inflammatory and Anti-Thrombotic Pharmaceutical Agents. Clin Exp Pharmacol 5: 192. doi:10.4172/2161-1459.1000192

References

1. Chakraborty S, Liao I-C, Adler A, Leong KW (2009) Electrohydrodynamics: A facile technique to fabricate drug delivery systems. Adv Drug Deliv Rev 6: 1043–1054.
2. Gryshkov O, Pogozhykh D, Zernetsch H, Hofmann N, Mueller T, et al. (2014) Process engineering of high voltage alginate encapsulation of mesenchymal stem cells. Mater Sci Eng C 36: 77–83.
3. Szentivanyi AL, Zernetsch H, Menzel H, Glasmacher B (2011) A review of developments in electrospinning technology: New opportunities for the design of artificial tissue structures. Int J Artif Organs 34: 986–997.
4. Zernetsch H, Repanas A, Gryshkov A, Al Halabi F, Rittinghaus T, Wienecke S, et al. (2013) Solving Biocompatibility Layer by Layer: Designing Scaffolds for Tissues. Biomed Tech (Berl) 58: 2013-4065.
5. Sill TJ, von Recum HA (2008) Electrospinning: Applications in drug delivery and tissue engineering. Biomaterials 29: 1989–2006.
6. Jiang S, Jin Q, Agarwal S (2015) Template Assisted Change in Morphology from Particles to Nanofibers by Side-by-Side Electrospinning of Block Copolymers. Macromol. Mater. Eng 299: 1298-1305.
7. Frenot A, Chronakis IS (2003) Polymer nanofibers assembled by electrospinning. Curr Opin Colloid Interface Sci 8: 64–75.
8. Szentivanyi A, Chakradeo T, Zernetsch H, Glasmacher B (2011) Electrospun cellular microenvironments: Understanding controlled release and scaffold structure. Adv Drug Deliv Rev 63: 209–220.
9. Zhang YZ, Wang X, Feng Y, Li J, Lim CT, Ramakrishna S (2006) Coaxial Electrospinning of (Fluorescein Isothiocyanate-Conjugated Bovine Serum Albumin)-Encapsulated Poly(ε-caprolactone) Nanofibers for Sustained Release. Biomacromolecules 7: 1049–1057.
10. Sun G, Wei D, Liu X, Chen Y, Li M, et al. (2013) Novel biodegradable electrospun nanofibrous P (DLLA-CL) balloons for the treatment of vertebral compression fractures. Nanomedicine: NBM 9: 829-838.
11. Qiu L, Shao Z, Wang W, Wang F, Wang J, et al. (2014) Enhanced Cyclability of C/Lithium Iron Phosphate Cathodes with a Novel water-soluble lithium-ion binder. Electrochimica Acta 45: 11-18.
12. Saraf A, Lozier G, Haesslein A, Kasper FK, Raphael RM, et al. (2009) Fabrication of Nonwoven Coaxial Fiber Meshes by Electrospinning. Tissue Eng Part C Methods 15: 333–344.
13. Seyednejad H, Ji W, Yang F, van Nostrum CF, Vermonden T, et al. (2012) Coaxially Electrospun Scaffolds Based on Hydroxyl-Functionalized Poly(ε-caprolactone) and Loaded with VEGF for Tissue Engineering Applications. Biomacromolecules 13: 3650–3660.
14. Qiu L, Shao Z, Wang J (2013) Study on Synthesis, Rheological and Electrospinning Functional Materials of Carboxymethyl Cellulose Lithium (CMC-Li). Acta Chimica Sinica 71: 1521-1526.
15. Woodruff MA, Hutmacher DW (2010) The return of a forgotten polymer-Polycaprolactone in the 21st century. Prog Polym Sci 35: 1217–1256.
16. Kim TG, Lee DS, Park TG (2007) Controlled protein release from electrospun biodegradable fiber mesh composed of poly (ε-caprolactone) and poly (ethylene oxide). Int J Pharm 338: 276–283.
17. Zhang X, Shi Z, Fu W, Liu Z, Fang Z (2012) In vitro biocompatibility study of electrospun copolymer ethylene carbonate-ε-caprolactone and vascular endothelial growth factor blended nanofibrous scaffolds. Applied Surface Science 258: 2301-2306.
18. Xu B, Li Y, Fang X, Thouas GA, Cook WD et al. (2013) Mechanically tissue-like elastomeric polymers and their potential as a vehicle to deliver functional cardiomyocytes. J Mech. Behav. Biomed. Mater 28: 354-365.
19. Raghavan P, Lim D-H, Ahn J-H, Nah C, Sherrington DC, et al. (2012) Electrospun polymer nanofibers: The booming cutting edge technology. React Funct Polym 72: 915–930.
20. Zamani M, Prabhakaran MP, Ramakrishna S (2013) Advances in drug delivery via electrospun and electrosprayed nanomaterials. Int J Nanomedicine 8: 2997–3017.
21. Pfeiffer D, Stefanitsch C, Wankhammer K, Müller M, Dreyer L, et al. (2014) Endothelialization of electrospun polycaprolactone (PCL) small caliber vascular grafts spun from different polymer blends. J Biomed Mater Res A 102: 4500-4509.
22. Gaudio CD, Ercolani E, Galloni P, Santilli F, Baiguera S, et al. (2013) Aspirin-loaded electrospun poly(ε-caprolactone) tubular scaffolds: potential small-diameter vascular grafts for thrombosis prevention. J Mater Sci Mater Med 24: 523–532.
23. Yan S, Xiaoqiang L, Shuiping L, Xiumei M, Ramakrishna S (2009) Controlled release of dual drugs from emulsion electrospun nanofibrous mats. Colloids Surf B Biointerfaces 73: 376–381.
24. Nejati E, Mirzadeh H, Zandi M (2008) Synthesis and characterization of nano-hydroxyapatite rods/poly(l-lactide acid) composite scaffolds for bone tissue engineering. Compos Part Appl Sci Manuf 39: 1589–1596.
25. Guan J, Fujimoto KL, Sacks MS, Wagner WR (2005) Preparation and characterization of highly porous, biodegradable polyurethane scaffolds for soft tissue applications. Biomaterials 26: 3961–3971.
26. Bakar SK, Niazi S (1983) Stability of aspirin in different media. J Pharm Sci 72: 1024–1026.
27. Okutan N, Terzi P, Altay F. (2014) Affecting parameters on electrospinning process and characterization of electrospun gelatin nanofibers. Food Hydrocoll 39: 19–26.
28. Thompson CJ, Chase GG, Yarin AL, Reneker DH (2007) Effects of parameters on nanofiber diameter determined from electrospinning model. Polymer 48: 6913–6922.
29. Katti DS, Robinson KW, Ko FK, Laurencin CT (2004) Bioresorbable nanofiber-based systems for wound healing and drug delivery: Optimization of fabrication parameters. J Biomed Mater Res B Appl Biomater 70: 286–296.
30. Demir MM, Yilgor I, Yilgor E, Erman B (2002) Electrospinning of polyurethane fibers. Polymer 43: 3303–3309.
31. Sun B, Long YZ, Zhang HD, Li MM, Duvail JL, et al. (2014) Advances in three-dimensional nanofibrous macrostructures via electrospinning. Prog Polym Sci 39: 862–890.
32. Cramariuc B, Cramariuc R, Scarlet R, Manea LR, Lupu IG, et al. (2013) Fiber diameter in electrospinning process. J Electrost 71: 189–198.
33. Sarasam A, Madihally SV (2005) Characterization of chitosan–polycaprolactone blends for tissue engineering applications. Biomaterials 26: 5500–5508.
34. Elzubair A, Elias CN, Suarez JCM, Lopes HP, Vieira MVB (2006) The physical characterization of a thermoplastic polymer for endodontic obturation. J Dent 34: 784–789.
35. Grey CP, Newton ST, Bowlin GL, Haas TW, Simpson DG (2013) Gradient fiber electrospinning of layered scaffolds using controlled transitions in fiber diameter. Biomaterials 34: 4993–5006.
36. Stylianopoulos T, Bashur CA, Goldstein AS, Guelcher SA, Barocas VH (2008) Computational predictions of the tensile properties of electrospun fibre meshes: Effect of fibre diameter and fibre orientation. J Mech Behav Biomed Mater 1: 326–335.
37. Jiang S, Duan G, Chen L, Hu X, Ding Y, et al. (2015) Thermal, mechanical and thermomechanical properties of tough electrospun poly (imide-co-benzoxazole) nanofiber belts. J. Chem.
38. Blond D, Walshe K, Blighe FM, Khan U, Almecija D, et al. (2008) Strong, Tough, Electrospun Polymer–Nanotube Composite Membranes with Extremely Low Density. Adv. Funct. Mater 18: 2618-2624.
39. Miyajima M, Koshika A, Okada J, Kusai A, Ikeda M (1998) Factors influencing the diffusion-controlled release of papaverine from poly (l-lactic acid) matrix. J Controlled Release 56: 85–94.
40. Lam CXF, Savalani MM, Teoh S-H, Hutmacher DW (2008) Dynamics of in vitro polymer degradation of polycaprolactone-based scaffolds: accelerated versus simulated physiological conditions. Biomed Mater 3: